

Nanoscale Zeeman localization of charge carriers in diluted magnetic semiconductor-permalloy hybrids

Mona Berciu¹ and Boldizsár Jankó^{2,3}

¹*Department of Physics and Astronomy, University of British Columbia, Vancouver BC, V6T 1Z1, Canada*

²*Materials Science Division, Argonne National Laboratory, Argonne, Illinois 60439 and*

³*Department of Physics, University of Notre Dame, Notre Dame, Indiana 46556*

We investigate the possibility of charge carrier localization in magnetic semiconductors due to the presence of a highly inhomogeneous external magnetic field. As an example, we study in detail the properties of a magnetic semiconductor-permalloy disk hybrid system. We find that the giant Zeeman response of the magnetic semiconductor in conjunction with the highly non-uniform magnetic field created by the vortex state of a permalloy disk can lead to *Zeeman localized* states at the interface of the two materials. These trapped states are chiral, with chirality controlled by the orientation of the core magnetization of the permalloy disk. We calculate the energy spectrum and the eigenstates of these Zeeman localized states, and discuss their experimental signatures in spectroscopic probes.

PACS numbers: 73.20.-r, 75.50.Pp, 75.75.+a

Diluted magnetic semiconductors (DMS) based on III-V alloys doped with Mn have attracted a lot of interest recently, due to their relatively high Curie temperatures T_c (110 K for $\text{Ga}_{0.95}\text{Mn}_{0.05}\text{As}$) [1], below which they exhibit ferromagnetic order. In the ferromagnetic state, the charge carriers are spin-polarized, making these materials ideal sources of spin-polarized currents. To date, most suggested applications involving DMS are based on this property and therefore are restricted to operation in a range of temperatures $T \ll T_c$. On the other hand, in the paramagnetic phase $T > T_c$ both the $\text{III}_{1-x}\text{Mn}_x\text{V}$ and the more established $\text{II}_{1-x}\text{Mn}_x\text{VI}$ DMSs (which have even lower critical temperatures) show giant Zeeman response to external magnetic fields. In our opinion, this can lead to interesting applications in the paramagnetic state, and consequently at rather elevated temperatures.

Convincing experimental evidence for Zeeman splitting in the range of 30 meV for external fields of a few Tesla is provided by photoluminescence spectroscopy studies [2]. Even relatively small external magnetic fields of 0.1–0.5 T can easily lead to a 15 meV splitting of electronic energy levels [3]. Comparing this to the vacuum Zeeman splitting of ~ 0.06 meV (for $B = 0.5T$) suggests that the effective gyromagnetic ratio of charge carriers in diluted magnetic semiconductors is $g > 500$. The origin of this hugely enhanced Zeeman effect is attributed [3] to the strong magnetic coupling $\sum_i J_{sp-d}(\vec{r} - \vec{R}_i)\vec{s} \cdot \vec{S}_i$ between the spin \vec{s} of the charge carrier and the spins \vec{S}_i of the Mn located at \vec{R}_i . In the paramagnetic state, a small magnetic field \vec{B} induces a magnetization $\langle \vec{S}_i \rangle \sim \chi \vec{B}$ of the Mn spins, resulting in an effective Zeeman-like $\vec{s} \cdot \vec{B}$ coupling between the charge carrier spin and the magnetic field, in addition to the regular Zeeman coupling $-g_0\mu_B\vec{s} \cdot \vec{B}$ present in non-magnetic semiconductors. The scale of this additional coupling is set by the large exchange energy J_{sp-d} and results in a large effective g -value. This also implies that $g(T)$ has a strong

T -dependence through the magnetic susceptibility, and therefore can be tuned over a large range of values. This scenario is strongly supported by magneto-optical absorption measurements [4] of the Zeeman splitting at the band edge, which clearly exhibits a Brillouin-type dependence on the magnetic field.

The presence of giant Zeeman response in DMS implies that a moderate external magnetic field with a strong spatial variation on nanometer scale can be a very effective confining agent for spin-polarized charge carriers in these systems. Provided that such highly inhomogeneous external fields can be created and controlled adequately in a DMS, Zeeman-induced localization presents a new route for *manipulation of spin-polarized charge carriers at relatively high temperatures*.

Non-uniform magnetic fields with nanoscale spatial variations are known to appear in a variety of systems, such as the Abrikosov flux lattice [5] and arrays of nanoscale holes in superconducting films [6]. However, one of the most promising possibilities, which we investigate in this Letter, is provided by the magnetic vortex state [7] of nanoscale magnetic disks of ferromagnetic permalloy $\text{Ni}_{80}\text{Fe}_{20}$, Co or Fe. In the remanent state of such nanomagnets, the local magnetization near the perimeter of fairly thin disks has an in-plane vortex-like arrangement. This is energetically more favorable than a single ferromagnetic domain, since the exchange energy lost due to the gradual vortex rotation is more than compensated by the cancellation of the total dipole energy. This pattern is maintained for almost the entire volume of the disk. However, near the center of the disk, exchange interaction wins over dipole-dipole interaction and shape anisotropy, and the local magnetization is forced out of the plane of the disk. What is remarkable about this topological singularity in the magnetization is the extremely short length scales and high fields involved: Very recent experimental investigations indicate that the

radius of the magnetic core is about 30nm in permalloy disks [8, 9] and 10 nm in Fe disks [10], with maximum field values at the core in the 0.5-1.0 Tesla range. In this paper we show that such highly inhomogeneous magnetic fields provides a very effective localization agent for charge carriers in a system with large Zeeman effect.

We investigate the properties of magnetic disks for which the height d is small compared to radius R . In this limit, the disks exhibit vortex magnetization of the following general type [11]

$$\vec{M}(\vec{r}) = M_\phi(r)\vec{e}_\phi + M_z(r)\vec{e}_z \quad (1)$$

where cylindrical coordinates $\vec{r} = (r, \phi, z)$ are used. [Note that $r \neq |\vec{r}|$]. Using Maxwell's equations [12], we find the magnetic field created by a magnetization of the type described in Eq. (1). For the setup shown in Fig. 1, the magnetic field created in the DMS layer ($z > 0$) is $\vec{B}(\vec{r}) = \vec{b}(\vec{r}) - \vec{b}(\vec{r} + d\vec{e}_z)$, where, in cylindrical coordinates $\vec{r} = (r, \phi, z)$:

$$b_r(r, z) = \frac{\mu_0}{2\pi r} \int_0^{\rho_c} \frac{d\rho \rho M_z(\rho)}{\sqrt{(r+\rho)^2 + z^2}} \{K(f(r, \rho, z))$$

$$-E(f(r, \rho, z)) \cdot [\rho^2 + z^2 - r^2] \cdot [(r-\rho)^2 + z^2]^{-1}\} \quad (2)$$

$$b_\phi(r, z) = 0 \quad (3)$$

and

$$b_z(r, z) = \frac{\mu_0 z}{\pi} \int_0^{\rho_c} \frac{d\rho \rho M_z(\rho)}{(r-\rho)^2 + z^2} \cdot \frac{E(f(r, \rho, z))}{\sqrt{(r+\rho)^2 + z^2}} \quad (4)$$

while the corresponding magnetic vector $\vec{A}(\vec{r}) = \vec{a}(\vec{r}) - \vec{a}(\vec{r} + d\vec{e}_z)$, in the Coulomb gauge $\nabla \cdot \vec{A} = 0$, is given by

$$a_r(r, z) = a_z(r, z) = 0 \quad (5)$$

and

$$a_\phi(r, z) = -\frac{\mu_0}{2\pi} \frac{z}{r} \int_0^{\rho_c} \frac{d\rho \rho M_z(\rho)}{(r+\rho)\sqrt{(r+\rho)^2 + z^2}} \times$$

$$\left[(r-\rho)\Pi\left(\frac{4r\rho}{(r+\rho)^2}, f(r, \rho, z)\right) + (r+\rho)K(f(r, \rho, z)) \right] \quad (6)$$

Here, $f(r, \rho, z) = \sqrt{(4r\rho)/[(r+\rho)^2 + z^2]}$ and the elliptic functions $K(k)$, $E(k)$ and $\Pi(\nu, k)$ are defined in Ref. 13. The fact that only $M_z(r)$ enters these equations is expected, since the field lines induced by $M_\phi(r)$ are closed, and therefore this component does not contribute to the magnetic field outside the magnetic disk. Recent micromagnetic simulations have shown [10, 14] that the magnetization inside the disk is well fitted by the simple parameterization [11, 15, 16]:

$$|M_z(r)|/M_0 = \begin{cases} (\rho_c^2 - r^2)/(\rho_c^2 + r^2) & , r \leq \rho_c \\ 0 & , r > \rho_c \end{cases} \quad (7)$$

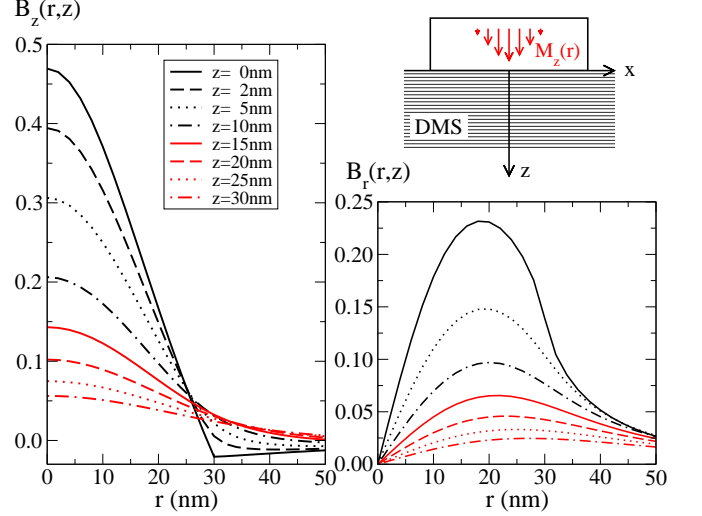


FIG. 1: $B_z(r, z)$ (left) and $B_r(r, z)$ (right) in units of $\mu_0 M_0 \approx 1$ T, plotted as a function of r for several values of z , for a disk of height $d = 50$ nm and a core radius $\rho_c = 30$ nm. The discontinuity in the slope of $B_z(r, 0)$ at $r = \rho_c$ is a consequence of the discontinuity of $dM_z(r)/dr$ at $r = \rho_c$ [see Eq. (7)].

and $|M_\phi(r)| = \sqrt{M_0^2 - M_z^2(r)}$. Such a structure is also known as a meron configuration in quantum Hall systems [17]. In permalloy disks, the saturation magnetization is $\mu_0 M_0 = 1.06$ T and the core radius $\rho_c \approx 30$ nm, if the disk radius $R \gg \rho_c$ [9]. [The core radius ρ_c decreases with decreasing d]. The core magnetization M_z has been observed experimentally in permalloy disks of typical height $d = 50$ nm and radii $R = 0.1 - 1 \mu\text{m}$ [8] as well as Fe disks with $d = 9$ nm and $R = 200 - 500$ nm [10].

Using Eqs. (2-4) and (7), we find the magnetic field created by the vortex inside the diluted magnetic semiconductor to have a typical profile as shown in Fig. (1). Inside the DMS layer, $B_z(r, z)$ is largest at $r = z = 0$, and decreases with increasing r and z . $B_r(r = 0, z) = 0$ as expected for a dipole-like field. However, $B_r(r, z)$ reaches a maximum value which is roughly half of the maximum $B_z(r, z)$ value for the same z , at a distance r of the order of ρ_c . The giant Zeeman effect present in the DMS systems leads to the possibility of trapping carrier states in the strong magnetic field near the disk surface.

The eigenstates of a charge carrier placed in such a magnetic field are given by the Schrödinger equation:

$$\left\{ \frac{1}{2m} [\vec{p} + q\vec{A}(\vec{r})]^2 - g\mu_B \frac{\vec{\sigma}}{2} \cdot \vec{B}(\vec{r}) \right\} \phi(\vec{r}) = E\phi(\vec{r}) \quad (8)$$

where, as already mentioned, the large g -factor effectively accounts for the magnetic exchange of charge carriers with locally magnetized Mn spins. The Hamiltonian given in Eq.(8) neglects electron-electron interactions. To first order, this is justified if the carrier concentration is either large enough that screening is very effective, or for low electron concentrations where only a small num-

ber of electrons might be trapped below each disk. In the latter case, Eq. (8) should accurately describe the strongest-bound state; for higher energy bound states, one should also include the screening provided by electrons occupying inner shells. We omit this complication here. Eq. (8) also assumes that the Mn spins create a smooth polarizing field for the electron, ignoring possible local fluctuations due to the fact that Mn spins are distributed randomly in the DMS. This so-called virtual crystal approximation has already been used extensively to describe DMS systems.

Given the symmetries of the magnetic and vector fields [Eqs. (2-6)], Eq. (8) has solutions of the following general form:

$$\phi_m(r, \phi, z) = \exp(im\phi) \begin{pmatrix} \phi_{\uparrow}^{(m)}(r, z) \\ \phi_{\downarrow}^{(m)}(r, z) \exp[i\phi] \end{pmatrix} \quad (9)$$

where the angular momentum m is an integer. The extra phase $\exp[i\phi]$ in the spin-down component has two significant consequences: (1) σ_z is not a good quantum number. [Besides the $\langle \hat{s}_z \rangle \neq 0$ part, the expectation value of the spin acquires a radial contribution $\langle \hat{s}_x + i\hat{s}_y \rangle \sim \exp(i\phi)$, for all m . This is clearly due to the existence of a radial part $B_r(r, z)$ in the magnetic field], and (2) the (usually expected) degeneracy between states with $\pm m$ is now lifted. The reason is that the presence of the magnetic field breaks the time-reversal symmetry responsible for this degeneracy. This has interesting consequences, as described below.

The general form of the wave function given above allows us to draw immediate conclusions regarding selection rules governing the electromagnetic response of the electronic states trapped in the DMS by the vortex magnetic field. Assume that the system is exposed to monochromatic radiation, and let $\vec{A}_L(\vec{r})$ and $\vec{B}_L(\vec{r}) = \nabla \times \vec{A}_L(\vec{r})$ be the vector potential, respectively magnetic field associated with it. Then the Schrödinger equation (8) acquires three extra terms, proportional to $\vec{\sigma} \cdot \vec{B}_L(\vec{r})$, $(\vec{p} + q\vec{A}) \cdot \vec{A}_L(\vec{r})$ and to $\vec{A}_L^2(\vec{r})$, in order of decreasing magnitude. Assume that the beam propagates along the z -axis and is circularly polarized, $\vec{B}_L^{(\pm)}(z) \sim (\vec{e}_x \pm i\vec{e}_y) \exp(ikz)$. Using Eq. (9) it is straightforward to find the selection rules $\langle m' | \vec{\sigma} \cdot \vec{B}_L^{(\pm)} | m \rangle \sim \delta_{m', m \pm 1}$. (The term $(\vec{p} + q\vec{A}) \cdot \vec{A}_L(\vec{r})$ obeys the same selection rules, while the $\vec{A}_L^2(\vec{r})$ term induces two-photon processes but with a vanishingly small probability [18]). This selection rule implies that the absorption of a right (left) circularly polarized photon excites the electron to a level with an m increased (decreased) by one unit. If levels with $\pm m$ are no longer degenerate, the system will interact differently with photons of different circular polarizations.

Let us now use a simplified model to demonstrate the lifting of the $\pm m$ degeneracy. First, the terms involving the vector field $\vec{A}(\vec{r})$ are removed from Eq. (8). This is justified since they are vanishingly small compared to the

Zeeman term, due to the supplementary enhancement of the later by the interaction with the Mn spins. Second, since we are interested in the most strongly-bound states, which are likely to be localized at small (r, z) values, we use Taylor series for the magnetic fields in this region, given (up to quadratic terms) by:

$$B_r(r, z) = \mu_0 M_0 B \left(\frac{z}{\rho_c} \right) \frac{r}{\rho_c}$$

$$B_z(r, z) = \mu_0 M_0 \left[A \left(\frac{z}{\rho_c} \right) - b_3 \frac{r^2}{\rho_c^2} \right]$$

where the functions

$$A(z) = b_1 - b_2 z + 2b_3 z^2 \quad \text{and} \quad B(z) = \frac{b_2}{2} - 2b_3 z$$

have been introduced for later convenience. These fields continue to satisfy the condition $\nabla \cdot \vec{B} = 0$, as necessary. The coefficients b_1, b_2 and b_3 are complicated functions of d/ρ_c . In the limit $d/\rho_c \rightarrow \infty$, we find $b_1 = 1/2$, $b_2 = (\pi + 2)/4$ and $b_3 = 1$. These asymptotic values turn out to give reasonable approximations for the typical experimental parameters $d = 50$ nm and $\rho_c = 10 - 30$ nm, with relative errors less than 10% for $d/\rho_c = 5/3$ and decreasing very fast to zero for larger ratios [19]. As a result, the asymptotic values will be used in the remainder of this paper.

With these simplifications, we look for eigenfunctions [see Eq. (9)] of the following form:

$$\phi_{\uparrow}^{(m)}(r, z) = a_1(z/\rho_c) \left(\frac{r}{\rho_c} \right)^{|m|} \exp\left(-\frac{r^2}{b^2 \rho_c^2}\right)$$

$$\phi_{\downarrow}^{(m)}(r, z) = a_2(z/\rho_c) \left(\frac{r}{\rho_c} \right)^{|m+1|} \exp\left(-\frac{r^2}{b^2 \rho_c^2}\right)$$

Both components are regular for $r \rightarrow 0$. The functions $a_1(z/\rho_c)$ and $a_2(z/\rho_c)$ are determined, in dimensionless units $z/\rho_c \rightarrow z$, by the set of coupled equations:

$$\left[\frac{4(|m|+1)}{b^2} - \frac{d^2}{dz^2} - \alpha A(z) \right] a_1 + \frac{s-1}{2} \alpha B(z) a_2 = e a_1 \quad (10)$$

$$\left(\frac{4}{b^4} - \alpha \right) a_1(z) + \frac{s+1}{2} \alpha B(z) a_2(z) = 0 \quad (11)$$

$$\left[\frac{4(|m|+s+1)}{b^2} - \frac{d^2}{dz^2} + \alpha A(z) \right] a_2 - \frac{s+1}{2} \alpha B(z) a_1 = e a_2 \quad (12)$$

$$- \left(\frac{4}{b^4} + \alpha \right) a_2(z) + \frac{s-1}{2} \alpha B(z) a_1(z) = 0 \quad (13)$$

Here, $s = 1$ if $m \geq 0$ and $s = -1$ if $m < 0$. We define the energy unit $E_0 = \hbar^2/(2m\rho_c^2)$ and use $e = E/E_0$, while $2\alpha = g\mu_B\mu_0 M_0/E_0$ is the ratio between

the maximum Zeeman energy and this energy unit. This number is rather large. If we use $\rho_c = 30$ nm and $\mu_0 M_0 = 1.06$ T (typical values for permalloy disks), $m = 0.5m_0$ (band value for heavy hole mass in GaAs) and use the estimated effective gyromagnetic factor to be $g = 500$, we find $|\alpha| \approx 175$.

If $s = +1$, we see from Eq. (13) that there is a non-trivial solution if and only if $4/b^4 = -\alpha$, which is possible if $\alpha < 0$. This is the case when $M_0 < 0$, i.e. the z -axis disk magnetization M_z points away from the DMS surface [20]. With $b^2 = \sqrt{4/|\alpha|}$, Eq. (11) has the solution $a_1(z) = \frac{1}{2}B(z)a_2(z)$. Using this in Eq. (12) we find $a_2(z) = \exp(-kz)$, where $k > 0$ is linked to the eigenenergy through $e_m = 2\sqrt{|\alpha|}(m+2) + \alpha \frac{(6-\pi)(10+\pi)}{128} - k^2$. Finally, Eq. (10) must be satisfied up to powers of z^0 (the magnetic fields, and therefore the functions a_1 and a_2 , are accurate only up to z^2 , meaning that the second derivative of a_1 is accurate only up to z^0). This gives $k = -0.321\sqrt{|\alpha|} + 0.127|\alpha|$ (with $k > 0$ satisfied for any $|\alpha| > 1.56$). In other words, up to a large negative constant the spectrum $e_m = 2\sqrt{|\alpha|m}$ is similar to that of a harmonic oscillator ($s = +1 \rightarrow m \geq 0$) [21]. For typical values for the vortex core radius and effective mass (constants which set the energy scale E_0 as given above), the level spacing is in the range of 3 – 6 meV, which should be accessible by most spectroscopic tools.

To summarize, for $M_z < 0$ we find only solutions with $s = +1$ or $m \geq 0$, proving that the $\pm m$ degeneracy is indeed lifted in this simplified case. For $M_z > 0$, the reverse is true; we find only solutions with $m < 0$. However, these simple solutions only hold for small values of m , where the wave-functions are localized at small r and z and the Taylor series for the magnetic fields are valid. To find the true spectrum, one must integrate Eq. (9) numerically for the full expression of the magnetic fields; this work is in progress and the results will be reported elsewhere [19]. We expect that the degeneracy between $\pm m$ eigenstates is lifted in the general case as well. As already discussed, this means that the system will interact differently with photons of different circular polarization, depending also on the orientation (sign of) the magnetic disk core magnetization M_z . Such a property may be useful in designing spintronic devices: the memory bit (M_z up or down) controls the properties of the trapped electronic states, and therefore the behavior of the whole device. Other geometries, such as lines of ordered disks, could be used to trap and transport electric currents with similar non-trivial spin properties.

In conclusion, we suggest a different route to creating spintronic devices that can operate *at room temperature*, by combining the giant Zeeman effect of diluted magnetic semiconductors in the paramagnetic state with the highly inhomogeneous magnetic field created by nanoscale permalloy disks, or other nano-patterned magnetic material structures. In particular, we have shown that electronic states can be trapped near the surface of

a magnetic disk. Their properties can be suitably tailored using various diluted magnetic semiconductors and various types of magnetic disks, as well as by varying the temperature (since the effective g-factor has significant temperature dependence). Since time-reversal symmetry is broken in the presence of the magnetic field, the system will interact non-trivially with any other system which has a definite chirality, such as circularly polarized light. To our knowledge, this is the first time that Zeeman-induced localization has been suggested and demonstrated theoretically, or that electronic states with such unusual spin-polarization have been derived. Experiments to test these are currently in progress [22].

Acknowledgements We thank Gyorgy Csaba, V. Novosad, M. Grimsditch, J. K. Furdyna and V. Metlushko for useful discussions. This research was supported by NSERC of Canada (M.B.) and by NSF NIRT award DMR 02-10519 and the Alfred P. Sloan Foundation (B.J.). We also gratefully acknowledge the hospitality of the Argonne National Laboratory (M.B. and B.J.) and the Aspen Center for Physics (M.B.), where parts of this work were carried out.

-
- [1] H. Ohno *et al.*, Appl. Phys. Lett. **69**, 363 (1996).
 - [2] See, for example, S. Lee *et al.*, Phys. Rev. B **61**, 2120 (2000) and references therein.
 - [3] J. Furdyna, J. Appl. Phys. **64**, R29 (1988).
 - [4] N. Dai *et al.*, Phys. Rev. B **50**, 18 153 (1994).
 - [5] S.J. Bending *et al.*, Phys. Rev. Lett. **65**, 1060 (1990)
 - [6] V. Metlushko *et al.*, Phys. Rev. B **59**, 603-607 (1999).
 - [7] R. P. Cowburn *et al.*, Phys. Rev. Lett. **83**, 1042 (1999).
 - [8] T. Shinjo *et al.*, Science **289**, 930 (2000).
 - [9] J. Raabe *et al.*, J. Appl. Phys. **88**, 4437 (2000).
 - [10] A. Wachowiak *et al.*, Science **298**, 577 (2002).
 - [11] A. Hubert and R. Schäfer, *Magnetic Domains* (Springer, Berlin, 1998).
 - [12] J. D. Jackson, *Classical Electrodynamics*, (John Wiley & Sons, 3rd edition, 1998).
 - [13] $E(k) = \int_0^{\frac{\pi}{2}} d\theta \sqrt{1 - k^2 \sin^2 \theta}$, $K(k) = \int_0^{\frac{\pi}{2}} d\theta [\sqrt{1 - k^2 \sin^2 \theta}]^{-1}$, $\Pi(\nu, k) = \int_0^{\frac{\pi}{2}} d\theta [\sqrt{(1 - k^2 \sin^2 \theta)} / (1 - \nu^2 \sin^2 \theta)]^{-1}$.
 - [14] Gyorgy Csaba, (unpublished).
 - [15] A. Aharoni, J. Appl. Phys. **68**, 2892 (1990).
 - [16] N. A. Usov and S. E. Peschany, J. Magn. Magn. Mater. **118**, L290 (1993).
 - [17] D. J. Gross, Nucl. Phys. B **132**, 439 (1978).
 - [18] If the beam is shined along the DMS surface (propagation in the xOy plane) transitions are allowed between any two states m and m' , i.e there are no selection rules.
 - [19] Mona Berciu and Boldizsár Jankó, (unpublished).
 - [20] $\alpha < 0$ is also realized if $M_z > 0$, but $g < 0$, i.e. charge carriers are antiferromagnetically coupled to Mn spins. In the following we use the convention that $g > 0$.
 - [21] Proper boundary conditions must be imposed before the exact eigenstates can be found. These depend on the nature of the DMS-permalloy interface.
 - [22] J. Furdyna *et al.*, (unpublished).